SSRG International Journal of Mechanical Engineering
ISSN: 2348-8360/ https://doi.org/10.14445/23488360/IJME-V12I10P101

Volume 12 Issue 10, 1-9, October 2025

Original Article

Enhancing Sustainable VCR Engine Operation Using Mahua Oil Methyl Ester with Thermal Barrier Coating

Gopal Radhakrishnan Kannan

Department of Mechanical Engineering, PSNA College of Engineering and Technology, Dindigul, Tamil Nadu, India.

Corresponding Author : grkgop@gmail.com

Received: 02 August 2025 Revised: 03 September 2025 Accepted: 04 October 2025 Published: 31 October 2025

Abstract - *In order to lower hazardous emissions and improve the diesel engine characteristics, there has been a recent push for appropriate alternative fuels and improved performance tactics. In order to analyze the diesel engine behavior with variable compression ratios, the combined effect of alternate fuel and thermal barrier-coated engine crown was studied. Using Mahua Oil Methyl Esters (MOME) with various Compression Ratios (CR) ranging from 17:1, 19:1, and 21:1 at various load circumstances, the performance, emission, and combustion characteristics of the thermal barrier-coated VCR engine were examined and contrasted with those of diesel and non-coated or standard engines. Based on observed results, the adiabatic engine with a higher compression ratio of 21 (CR21-AE-B100) demonstrated the following characteristics: a higher cylinder gas pressure of 61.7 bar, a higher heat release rate of 78.6 J/ºCA, a shorter ignition delay period of 9.8 ºCA, a maximum brake thermal efficiency of 28.12%, the lowest Brake Specific Fuel Consumption (BSFC) of 0.3423 kg/kW h, a maximum Nitric Oxide (NO) emission of 575 ppm, and lowest smoke opacity of 37.8%.*

Keywords - *Adiabatic coating, Bond coat, Top coat, Combustion and emission, Mahua oil methyl ester, Performance.*

1. Introduction

Due to climate change, the world has been experiencing flash floods, droughts, increasing sea levels, surface temperatures, unexpected, intense rainstorms, and other natural disasters for the past 20 years. The primary cause of this climate change is the harmful emissions from conventional fuels used in industries, automobile engines, and human-made activities, including carbon monoxide, carbon dioxide, nitrogen oxides, smoke, and Particle Matter (PM) [1].

To meet their energy demands and improve their economic standing, heavily populated nations like India rely on importing crude oil from the Middle East. Heavy-duty engines are used in India for both agricultural and transportation reasons [2, 3]. When diesel engines were used, dangerous emissions such as smoke, Unburned Hydrocarbons (UHC), Carbon Monoxide (CO), Carbon Dioxide (CO2), and Nitrogen Oxides (NOx) were released. These emissions have a negative impact on the human respiratory system and contribute to climate change. Therefore, in order to achieve strict emission standards without sacrificing engine performance, it is necessary to find innovative ways to employ alternative fuels in diesel engines and engine modification tactics.

By varying engine parameters such as injection timing, pressure, compression ratio, and adiabatic or thermal barrier coating, the majority of researchers are creating biodiesel from different feedstocks and attempting to improve diesel engine performance. Poor viscosity, volatility, injector coking, and poor atomisation characteristics were among the key issues with using edible or non-edible oils in diesel engines [4]. Therefore, the only method to improve the viscosity, volatility, and atomisation properties of biodiesel is to transesterify the non-edible oils. One of the alternatives for traditional diesel in meeting the world's energy needs and reducing dangerous emissions is biodiesel [5, 6]. With the exception of its low emission profile and heating value, biodiesel has been shown to be a dependable alternative to traditional diesel.. Non-edible feedstocks such as mahua, karanja, neem, jatropha, rubber, linseed, pomegranate seed, and lemon peel oil can be used to create biodiesel, hence avoiding confrontation with the food crisis [7-13].

Additional research showed that combining thermal barrier-coated diesel engine parts and biodiesel improved the engine behaviour. Sharad P. Jagtap et al. (2020) studied the characteristics of a low heat rejection engine with Jatropha biodiesel. In their investigation, 250µm mullite material (Metco 6150) was applied to the piston crown surfaces. When compared to engines that were not coated, the results showed a lower emission profile. However, mixing biodiesel and 5% anhydrous ethanol to create the E05B10 mixture resulted in a further improvement in performance and reduced emission profile [14]. Karthickeyan et al. (2020) studied a single cylinder direct injection diesel engine with pomegranate seed biodiesel (B20). The plasma spray coating method was used to determine that Yttria Stabilised Zirconia (YSZ) was TBC. Because of its higher cylinder temperature, B20 demonstrated greater thermal efficiency in both CE and TBCE at high compression ratios, injection pressures, and injection timings. [15].

Curry leaf (Murraya koenigii) biodiesel was used by Karthickeyan Viswanathan et al. (2020) to study a Thermal barrier-covered combustion chamber on a diesel engine. B25-fueled coated engines demonstrated improved thermal efficiency of 0.49%. Additionally, the ceramic-coated engine was found to have improved combustion characteristics [16]. Using Moringa oleifera biodiesel, Karthickeyan (2019) examined the behaviour of YSZ-coated diesel engines. It was found that the coated engine had superior engine qualities [17].

The importance of using TBC to improve combustion characteristics by serving as a thermal insulating layer and consuming energy inside the combustion chamber was covered by Öztürk et al. (2019). When employing low heating value biodiesel, this calculated tactic was used to enhance engine performance [18].

Abbas et al. (2018) used a combination of biodiesel and pyrogallol to analyse a YSZ-coated engine. Compared to uncoated engine characteristics, it displayed superior engine characteristics. The coating materials, such as zirconia, zirconia with aluminium oxide, and fused zirconia, were examined to expand the study. At all load situations, fused zirconia outperformed the other two chosen coating materials [19].

Using warmed linseed oil, Yilmaz and Gumus (2014) investigated Lombardini 6LD400 diesel engines under both conventional and ceramic-coated engine settings. It was noted that the greater combustion temperature resulted in improved engine performance for the Cr_3C_2-coated engine [20]. The influence of TBC on diesel engines with waste cooking oil biodiesel–diesel blends was documented by Selman Aydın and Cenk Sayın (2014). In their investigation, a base layer of 100 µm NiCrAl was coated on the piston, intake, and exhaust valves. A 400 µm top coating material consisting of a blend of 88% ZrO_2, 4% MgO, and 8% Al_2O_3 was also applied. With Nitrogen Oxide (NOx) emissions excluded, the results showed that the coated engine exhibited a reduction in both the emission profile and Brake-Specific Fuel Consumption (BSFC). Additionally, the coated engines showed higher cylinder gas pressure and Heat Release Rate (HRR [21].

According to Buyukkaya and Cerit (2008), the use of thermal barrier coatings resulted in improved combustion characteristics, reduced emissions, lower fuel consumption, and increased thermal efficiency [22]. Investigation of TBC on the engine using the plasma spray approach was covered by Parlak A. (2005). The negative impacts of wear, corrosion, oxidation, and friction were generally lessened in the ceramic-coated parts with improved engine performance characteristics[23].

1.1. Statement of Novelty

According to the literature review, when utilising biodiesel with or without engine modifications, thermal barrier-coated engine parts can lower heat rejection, enhance thermal efficiency, improve combustion characteristics, and reduce emission profiles. However, the combined impact of TBC and changing engine settings with biodiesel was limited.

Additionally, only a small number of researchers used Mahua Oil Methyl Esters (MOME), which were made from Mahua oil that was readily available in India, to study diesel engines. These studies did not cover the concurrent impact of modifying engine operating conditions and applying a heat barrier coating. Therefore, utilising Mahua Oil Methyl Esters (MOME), an attempt was made to examine the combined effect of the TBC piston crown of a variable compression ratio diesel engine. The obtained results were related to both diesel and non-coated engines.

2. Materials and Methods

Transesterification was used in the study to turn Mahua oil into biodiesel. By changing the compression ratios from 17:1 to 21:1 in increments of 2, the performance, emissions, and combustion characteristics of a single-cylinder, four-stroke direct-injection diesel engine were examined using biodiesel. The outcomes were contrasted with those of a TBC engine.

2.1. Biodiesel Production

Due to higher oil content and accessibility among other feed stocks, Mahua oil was selected for the synthesis of biodiesel [24, 25]. At room temperature, it seemed semisolid and yellow. Two-stage transesterification procedures were chosen to turn raw Mahua oil into biodiesel. The first step involved adding methanol and highly concentrated H2SO4 to raw oil at about 55 °C for two hours. In the second step, the catalyst KOH and reactant methanol were combined with the leftover oil. For two hours, the mixture was heated to around 55 °C.

The second stage products were allowed to be washed with water to remove moisture and excess methanol from the Mahua Oil Methyl Ester (MOME), and the residual oil was heated to about 110 °C. MOME was mixed in different amounts with regular diesel, ranging from 20% to 80%. The fuel characterization of MOME and its blends with diesel was determined as per the ASTM D6751 standard. Table 1 displays the physical-chemical characteristics of diesel, MOME, and its blends, along with raw Mahua Oil (MO)

Table 1. Fuel properties of Diesel Mahua Oil, MOME, and its blends

Fuel Properties	Diesel	Mahua Oil	B20	B40	B60	B80	B100 /MOME	ASTM Standard
Density (kg/m^3) at 27^{o}C	851	925	858	865	872	879	886	ASTM D1298
Kinematic Viscosity @ 40°C	2.432	24.58	2.780	2.989	3.258	3.742	4.329	ASTM D445
Calorific value MJ/kg	42.08	36.23	41.30	40.53	39.75	38.97	38.20	ASTM D40
Flash Point °°C	42	232	101	108	114	123	130	ASTM D93
Cetane index	55	57	48.3	50.3	52.3	54.0	61	ASTM D976
Copper Strip corrosion	1a	1a	1a	1a	1a	1a	1a	ASTM D130

According to ASTM D1298, the fuel blend's density was calculated and found to be within acceptable bounds. The MOME, or biodiesel, had a lower heating value than diesel but a higher one than raw Mahua oil. MOME and its blends showed a higher flash point for safer handling and storage. The biodiesel exhibited a slightly higher Cetane index or better ignition quality. One consequence of corrosiveness on copper engine components is the corrosion of copper strips. MOME and its blends displayed a slightly tarnished strip that was identified as "1a" and nearly identical to a freshly polished strip.

2.2. Thermal Barrier Coating or Adiabatic Coating

Because the coated engine reduces heat transmission in the combustion chamber, it is more reliable and durable than a regular or non-coated engine, leading to improved engine performance. The engine valve, piston crown, and cylinder head can all be affected by TBC [26]. This work used the plasma spray coating process to cover the piston crown with a 150 µm thick NiCrAl (Nickel-Chromium-Aluminum) bond coat and a 200 µm thick top coat of Yttria (Y_2O_3)-stabilized Zirconia (ZrO_2) (YSZ). A preliminary study was used to determine the thickness and composition of a suitable adiabatic coating. Figure 1 displays TBC TBC-coated piston crown.

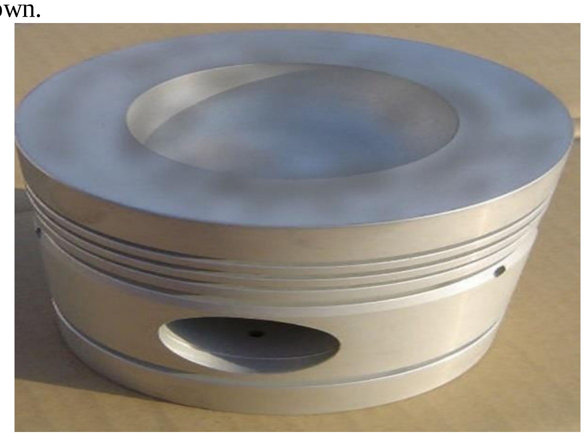

Fig. 1 TBC coated piston crown

2.3. Experimental Setup and Methodology

The line diagram and photographs of the experimental setup are shown in Figures 2 and 3. A single-cylinder, four-stroke, variable compression ratio multifuel engine with an eddy current dynamometer was considered for the study. Technical specifications of the diesel engine are given in Table 2. In the current investigation, the cylinder head can be raised or lowered to alter the compression ratio. This affects the clearance volume that is obtained.

Fig. 2 Photo of test engine setup

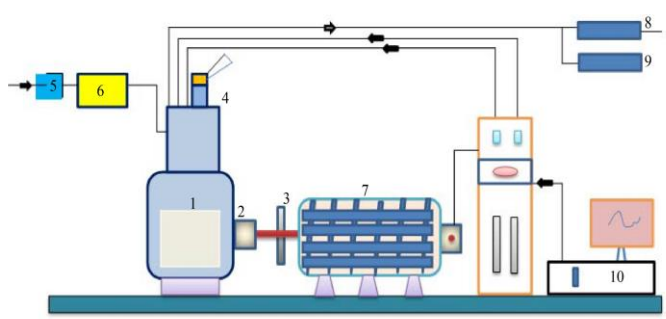

Fig. 3 Schematic diagram of experimental setup

1. Diesel Engine, 2. Angle encoder, 3. Balancing wheel, 4. Knob for VCR, 5. Intake Filter, 6. Air Storage Tank, 7. Inductor dynamometer, 8. AVL 5 Gas Instrument, 9. Opacity tester, 10. DAS, 11. Engine Foundation

Using MOME or B100, experimental tests were carried out for Standard or non-coated Engines (SE) and TBC coated or Adiabatic Engines (AE) at various compression ratios between 17:1, 18:1, and 21:1 under varying load circumstances ranging from 0% to 100% with increments of 25%. All of the measuring devices were checked, adjusted, and calibrated through a series of trial tests. Engine behaviours of different fuels at a steady 1500 rpm with varied loads and compression ratios were all covered in the engine study.

The results of this study's use of MOME to modify the compression ratios of adiabatic or TBC-coated engines were compared to those of the normal or non-coated engine.

Table 2. Technical specification of VCR engine

General Details	Computerized VCR Single Cylinder Four Stroke Engine (Multiple Fuel)
Rated Power	5.2. kW at 1500 rpm
Compression Ratio	Variable from 5:1 to 22:1
Bore	80 mm
Stroke	110 mm
Type of fuel	Multiple fuel
Loading	Inductor Dynamometer
Temperature Sensor	Type K- Chromel thermocouples
Make of the engine	Kirloskar
Starting	Self-starter
Cooling	Water

3. Results and Discussion

3.1. Performance Characteristics

3.1.1. Brake Thermal Efficiency

Figure 4 shows the Braking Thermal Efficiency (BTE) of the Standard Engine (SE) and Adiabatic Engine (AE) utilising biodiesel or MOME under various load circumstances and compression ratios. When CR17-AE-Diesel was compared to CR17-SE-Diesel, a higher brake thermal efficiency of 28.12% was achieved, mostly by the thermal barrier-coated piston crown. B100's brake thermal efficiency was worse than diesel's, regardless of the engine's CR, standard operating conditions, or adiabatic operation.

This is mostly because of biodiesel's lower net calorific value than diesel [27]. It was found that raising the compression ratio from 17:1 to 21:1 improved the braking thermal efficiency of biodiesel. The CR21-AE-Biodesel demonstrated the highest brake thermal efficiency of 26.98% under 100% load conditions.

The TBC piston crown improved combustion by raising the temperature and increasing the compression ratio, which in turn improved atomisation within the combustion chamber.

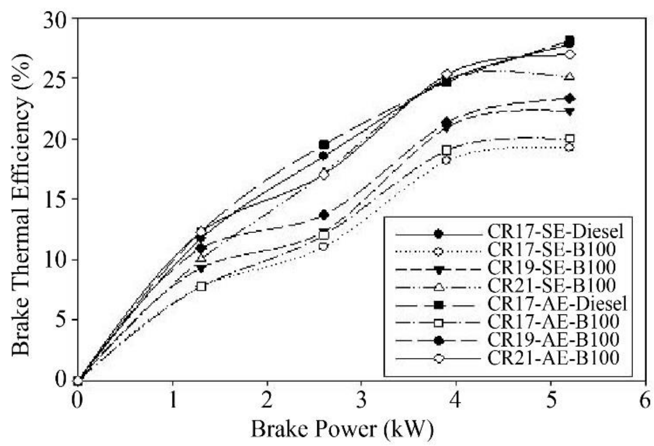

Fig. 4 Variation of BTE for test fuels

3.1.2. Brake Specific Fuel Consumption (BSFC)

The Brake-Specific Fuel Consumption (BSFC) of test fuel under various engine settings, loads, and compression ratios is shown in Figure 5. As load conditions increased, B100 demonstrated a decrease in BSFC. Due to the increased calorific value of diesel, a minimum BSFC of 0.30 kg/kW h was recorded for CR17-AE-Diesel. With 100% load conditions, the CR21-AE-B100 and C21-SE-B100 showed the lowest BSFCs of 0.34 kg/kW h and 0.36 kg/kW h, respectively. The higher resistance to flow and poor heating value of MOME were offset by the thermally coated piston crown and enhanced compression ratio. However, compared to CR21-SE-B100 and CR21-AE-B100, the BSFC of CR19-SE-B100 and CR19-AE-B100 had somewhat higher values. This is mostly due to the engine's insufficient compression ratios, which led to subpar atomisation.

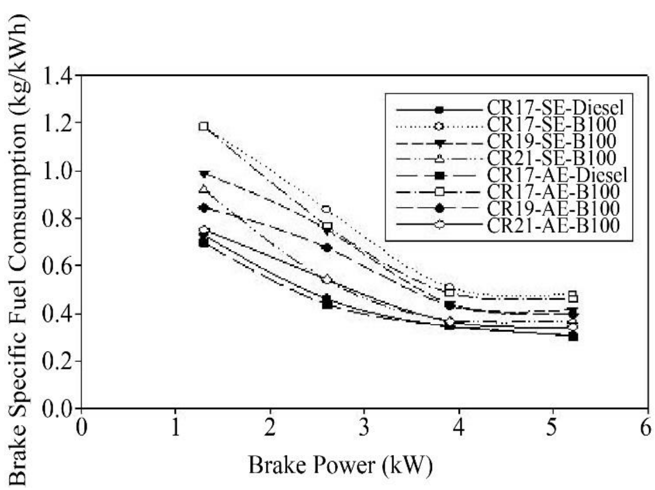

Fig. 5 BSFC of test fuels for various compression ratios and load conditions

3.2. Emission Characteristics

3.2.1. Carbon Monoxide (CO) Emission

Figure 6 shows the Carbon Monoxide (CO) emissions from biodiesel at different compression ratios, normal engines, and adiabatic engines with brake power.

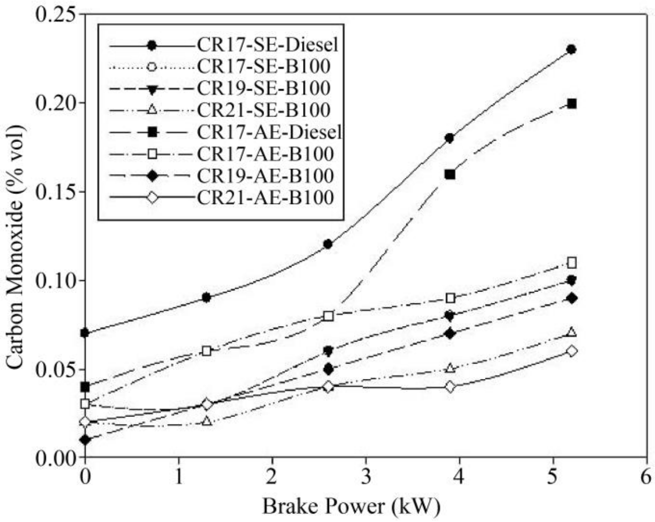

Fig. 6 Carbon Monoxide (CO) emission of test fuels

As load conditions increase, so do the CO emissions from diesel and biodiesel. Under 100% load conditions, maximum CO emissions from CR17-SE-Diesel and CR17-AE-Diesel were 0.23% Vol and 0.2% Vol, respectively. Despite having a piston crown that has been thermally treated, diesel emits the most CO since it has no oxygen. The impact of biodiesel viscosity on fuel spray properties is responsible for the elevated CO emissions of biodiesel under different load circumstances [30]. At 100 load conditions, the CR21-AE-B100 produced the lowest CO emission of 0.06% Vol due to a higher compression ratio and an adiabatic engine. This is explained by the increased temperature brought on by the higher compression ratio of 21 and an adiabatic engine.

3.2.2. Carbon Dioxide (CO_2) Emission

Carbon Dioxide (CO_2) emissions of diesel and biodiesel under various load circumstances and compression ratios are illustrated in Figure 7. At 100% load conditions, the maximum CO_2 emissions for CR17-SE-Diesel and CR17-AE-B100 were 4.3% and 4.5%, respectively.

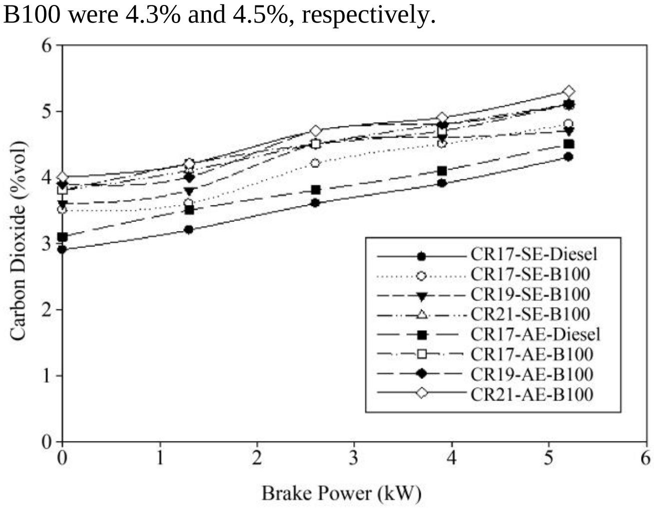

Fig. 7 CO_2 emission of test fuels for various compression ratios, SE, AE, and load conditions

Because of greater temperatures in the cylinder and the higher oxygen content of biodiesel, test fuels' CO_2 emissions are rising as load and compression ratios increase. The thermally coated engine emitted more CO_2 than the uncoated engine.

With a maximum CO_2 emission of 5.3% Vol, CR21-AE-B100 outperformed CR17-SE-Diesel and CR21-SE-B100 by 1% and 0.2%, respectively. This is because the adiabatic engine with B100 or the increased compression ratio of 21 both contributed to improved combustion.

3.2.3. Unburnt Hydrocarbon (UHC) Emission

Figure 8 displays the UHC emission of test fuels under conventional and adiabatic engine conditions with different compression ratios and load circumstances. Under different load settings, test fuels' UHC emissions are rising.

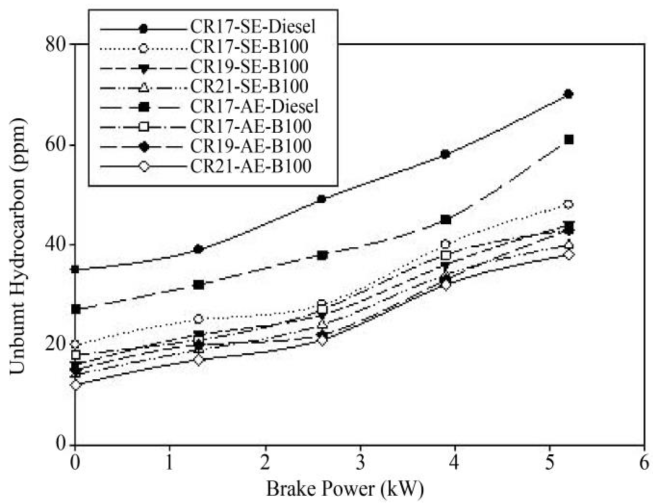

Fig. 8 UHC emission of test fuels

Figure 8 demonstrates that, regardless of whether an engine is adiabatic or conventional, diesel emits more Unburnt Hydrocarbon (UHC) than biodiesel. Because of the greater exhaust temperature caused by the higher cylinder temperature, thermal barrier-coated engines demonstrated decreased UHC emissions of test fuels.

Maximum load conditions, lower UHC emission of 38 ppm for CR21-AE-B100. This is due to higher temperature and the TBC piston crown, all of which improve combustion.

3.2.4. Nitric Oxide (NO) Emission

Nitric Oxide (NO) emission for different test fuel compression ratios and loads is given in Figure 9.

The increment in NO emission can be explained by a TBC piston crown, a greater compression ratio from 17 to 21, faster, improved combustion, and a greater cylinder gas temperature as a result of peak pressure [28, 29].

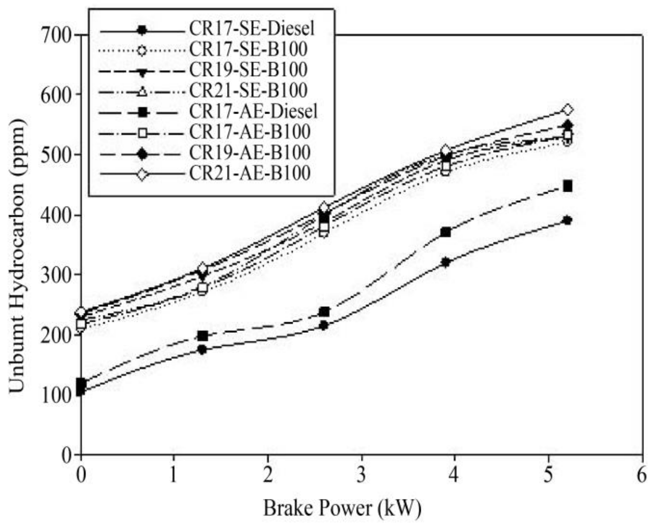

Fig. 9 NO emission with various compression ratios and load conditions

Maximum NO emission of 575 ppm was observed for CR21-AE-B100 at 100% load condition because biodiesel contains more oxygen and is heated to a higher temperature at an advanced compression ratio.

3.2.5. Smoke Emission

Smoke opacity of test fuels at various load circumstances and compression ratios is presented in Figure 10. CR21-AE-B100 showed the lowest smoke opacity, measuring 37.8%.

Because biodiesel has a larger oxygen content and burns better at higher compression ratios, it results in higher gas temperature [30], leading to improved combustion. When compared to non-coated engines, this could explain why test fuels like CR17-AE-B100 and CR19-AE-B100 had lower smoke levels.

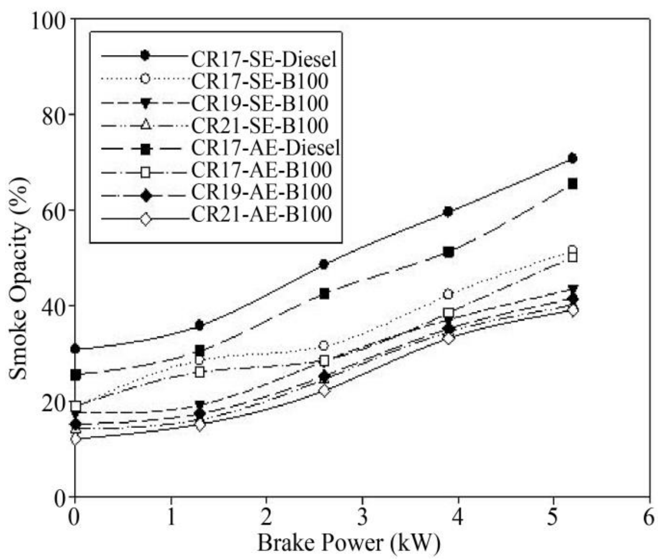

Fig. 10 Smoke opacity for different compression ratios and load conditions

3.2.6. Exhaust Gas Temperature

Figure 11 displays the Exhaust Gas Temperature (EGT) of diesel and biodiesel under different load situations and compression ratios. Under various compression ratios, load conditions, and coated and non-coated engine settings, biodiesel's EGT is lower than that of diesel's due to low net heating value; the exhaust gas temperature decreases with a higher compression ratio [31]. The CR21-AE-B100 test fuel had the lowest exhaust gas temperature, measuring 198 °C. This is explained by the possibility of improved performance due to a lower exhaust gas temperature [32].

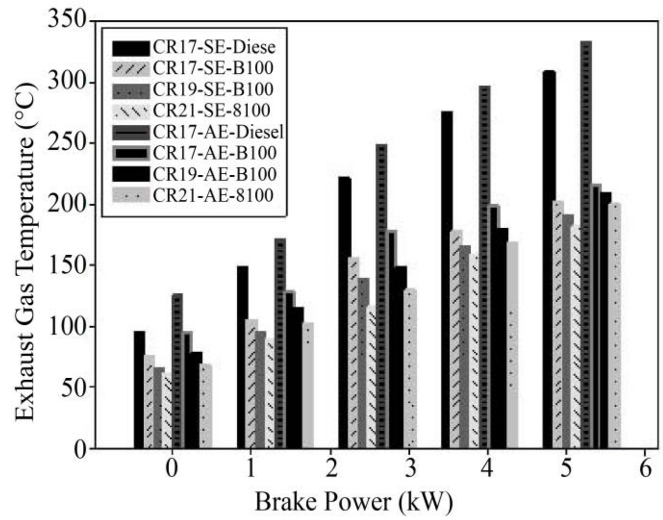

Fig. 11 EGT of test fuels for different compression ratios

3.3. Combustion Characteristics

3.3.1. Cylinder Pressure

Figure 12 shows the cylinder pressure with the crank angle for standard, adiabatic engines operating at 100% load circumstances, as well as test fuels with different compression ratios.

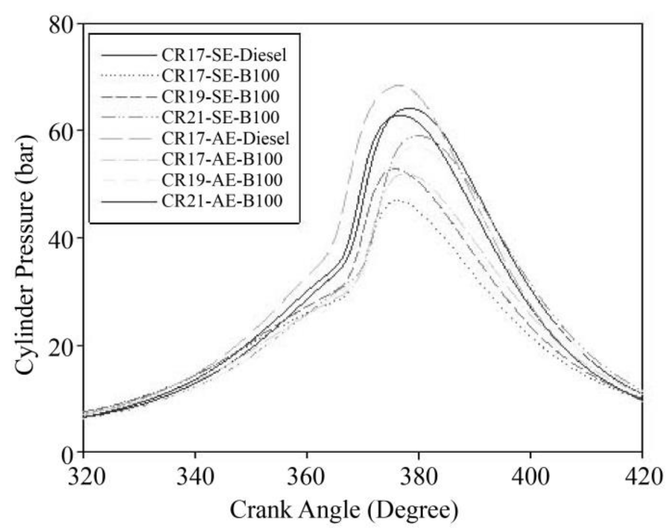

Fig. 12 Cylinder pressure of test fuels

Due to improved combustion, the cylinder pressure increased as the compression ratio surged. Additionally, for all test fuels, the adiabatic engine displayed somewhat higher cylinder pressure than the SE operation. Because conventional diesel has a higher calorific value, CR17-AE and CR17-SE diesel were found to have maximum cylinder pressures of 67.54 bar and 63.27 bar, respectively. CR21-AE-B100 achieved a cylinder pressure of 61.7 bar, 5.6% higher than CR21-SE-B100. This is mostly due to the greater gas temperature produced by an adiabatic piston crown.

3.3.2. Cylinder Gas Peak Pressure

The cylinder gas peak pressure of test fuels under various load circumstances and compression ratios is shown in Figure 13. The cylinder gas peak pressures for CR17-SE-B100 and CR19-SE-B100 were found to be 33.7 bar and 35.2 bar, respectively, under low load conditions. Additionally, the biodiesel-fueled AE displayed lower cylinder gas peak pressures of 34.7 bar and 37.4 bar at lower compression ratios of 17 and 19.

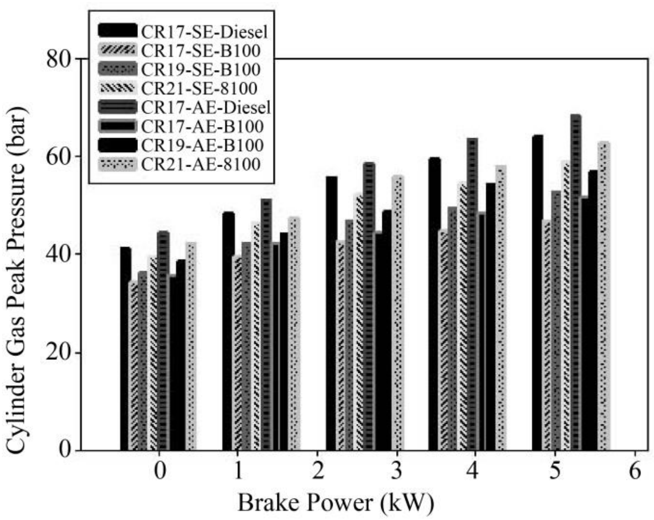

Fig. 13 Variation of cylinder gas peak pressure of test fuels

However, the CR21-SE-B100 and CR21-AE-B100 displayed a slightly lower cylinder gas peak pressure when compared to diesel fuel during SE and AE operation.

3.3.3. Heat Release Rate

Heat Release Rate (HRR) of test fuels with the varying crank angles is presented in Figure 14. Biodiesel demonstrated a lower HRR across the whole compression ratio range, regardless of SE and AE circumstances. For CR21-AE-B100, the maximum heat release rate was recorded at 78.6 J/ºCA.

This is because the lower heating value, the oxygen component of MOME, along with advanced compression ratio and TBC, caused it to release heat at a faster pace. However, under 100% load conditions, the CR21-SE-B100 demonstrated a higher heat release rate of 77.5 J/ºCA than the CR21-AE-B100.

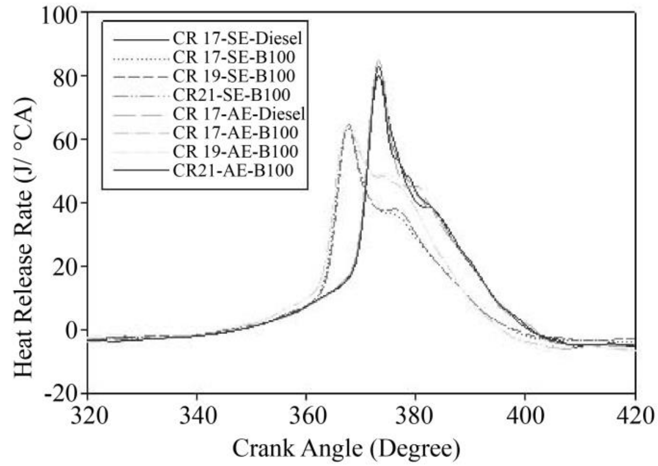

Fig. 14 Variation of the heat release rate of test fuels

3.3.4. Ignition Delay

The Ignition Delay (ID) duration of MOME and diesel under different load circumstances and compression ratios is shown in Figure 15. As loads increase, diesel and biodiesel's ignition delay times shorten. When compared to diesel, biodiesel had a shorter ignition delay period, as can be seen from the figure, a thermal barrier-coated engine that reduces ignition delay for all test fuels due to improved combustion [28].

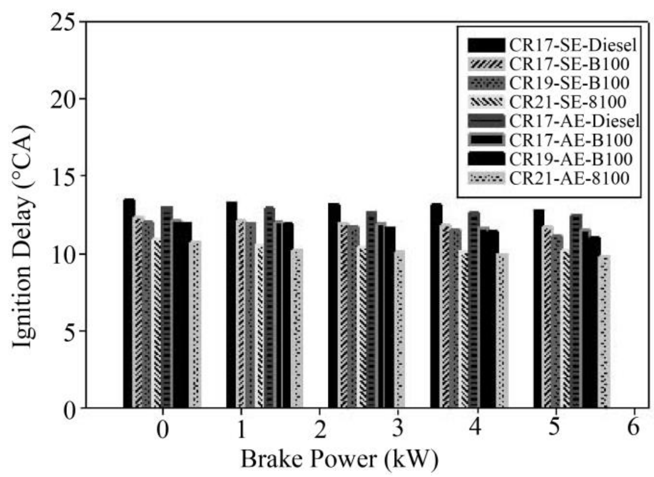

Fig. 15 ID of test fuels at various compression ratios and loads

CR21-AE-B100 had the smallest ignition delay duration (9.5 ℃), which is less than that of the CR21-SE-B100 at the maximum load condition due to lessened Physical delay by the combined effect of higher CR and an adiabatic engine that raised the gas temperature.

4. Conclusion

In this work, the trans-esterification procedure was used to prepare the biodiesel, or MOME. According to ASTM guidelines, the fuel attributes of MOME blends and MOME were investigated and contrasted with those of conventional fuel. The following engine features were noted based on research findings:

- Compared to CR17-SE-Diesel, CR17-AE-Diesel had a maximum brake thermal efficiency of 28.12%. When powered by biodiesel, adiabatic or thermal barrier-coated engines showed a significant increase in brake thermal efficiency.
- CR17-AE-Diesel had the BSFC of 0.30 kg/kW h, which is slightly lower than that of CR17-SE-Diesel. At maximum load conditions, the C21-AE-B100 and C21-SE-B100 showed the lowest BSFC of 0.34 kg/kW h and 0.36 kg/kW h across different compression ratios.
- The highest CO_2 emission of 5.3% Vol was observed for CR21-AE-B100, which is 0.2% and 1% more than that of CR21-SE-B100 and CR17-SE-Diesel. At maximum load, CR21-AE-B100 achieved a minimum UHC emission of 38 ppm. A maximum NO emission of 575 ppm was recorded with the CR21-AE-B100. The lowest smoke opacity of 37.8% was displayed by CR21-AE-B100.
- The CR21-AE-B100 recorded a cylinder pressure of 61.7 bar, 5.6% greater than the CR21-SE-B100.
- CR21-AE-B100 achieved the highest heat release rate of 78.6 J/ºCA Under conditions of 100% load, the CR21-AE-B100 displayed the smallest ignition delay duration, 9.8 ºCA.

In comparison to a non-coated engine using conventional diesel, an adiabatic or thermal barrier-coated engine with MOME demonstrated improved engine performance at a CR of 21. Additionally, MOME combined with TBC and VCR engines offers a good option for power plants and automobiles looking for an environmentally responsible and sustainable substitute for traditional diesel. Through environmentally friendly, energy-efficient engine settings, the study supports the industry's energy demands, particularly for applications in heat engines and decentralised power production, where MOME utilization is becoming more popular. Additionally, the results of the study open the door for the creation of energy-efficient, flex-fuel, and sustainable cleaner diesel engines.

References

[1] Frederica Perera, “Pollution from Fossil-Fuel Combustion is the Leading Environmental Threat to Global Pediatric Health and Equity: Solutions Exist,” *International Journal of Environmental Research and Public Health*, vo. 15, no. 1, pp. 1-16, 2018. [CrossRef] [Google Scholar] [Publisher Link]

[2] N.I.T.I. Aayog, “*Rocky Mountain Institute 2018 Goods on the Move: Efficiency & Sustainability in Indian Logistics*,” Technical Report, 2018. [Google Scholar]

[3] “*Renewables 2019 Global Status Report*,” pp. 1-336, 2019. [Google Scholar] [Publisher Link]

[4] S. Kerschbaum, and G. Rinke, “Measurement of the Temperature Dependent Viscosity of Biodiesel Fuels,” *Fuel*, vol. 83, no. 3, pp. 287-291, 2004. [CrossRef] [Google Scholar] [Publisher Link]

[5] S.N. Naik et al., “Production of First and Second Generation Biofuels: A Comprehensive Review,” *Renewable & Sustainable Energy Reviews*, vol. 14, no. 2, pp. 578-597, 2010. [CrossRef] [Google Scholar] [Publisher Link]

[6] Alison Mohr, and Sujatha Raman, “Lessons from First Generation Biofuels and Implications for the Sustainability Appraisal of Second Generation Biofuels,” *Energy Policy*, vol. 63, pp. 114-122, 2013. [CrossRef] [Google Scholar] [Publisher Link]

[7] R. Piloto-Rodríguez et al., “Conversion of by-Products from the Vegetable Oil Industry into Biodiesel and its Use in Internal Combustion Engines: A Review,” *Brazilian Journal of Chemical Engineering*, vol. 31, no. 2, pp. 287-301, 2014. [CrossRef] [Google Scholar] [Publisher Link]

[8] Ayyasamy Tamilvanan et al., “Effect of Diethyl Ether and Ethanol as an Oxygenated Additive on Calophyllum Inophyllum Biodiesel in CI Engine,” *Environmental Science and Pollution Research*, vol. 28, pp. 33880-33898, 2021. [CrossRef] [Google Scholar] [Publisher Link]

[9] K. Nanthagopal, B. Ashok, and R. Thundil Karuppa Raj, “Influence of Fuel Injection Pressures on Calophyllum Inophyllum Methyl Ester Fuelled Direct Injection Diesel Engine,” *Energy Conversion and Management*, vol. 116, pp. 165-173, 2016. [CrossRef] [Google Scholar] [Publisher Link]

[10] B. Ashok et al., “Calibration of Idling Characteristics for Lemon Peel Oil Using Central Composite Design in Light Commercial Vehicle Diesel Engine,” *Energy Conversion and Management*, vol. 221, 2020. [CrossRef] [Google Scholar] [Publisher Link]

[11] A.M. Ashraful et al., “Production and Comparison of Fuel Properties, Engine Performance, and Emission Characteristics of Biodiesel from Various Non-Edible Vegetable Oils: A Review,” *Energy Conversion and Management*, vol. 80, pp. 202-228, 2014. [CrossRef] [Google Scholar] [Publisher Link]

[12] Selman Aydin, Cenk Sayin, and Hüseyin Aydin, “Investigation of the Usability of Biodiesel Obtained from Residual Frying Oil in a Diesel Engine with Thermal Barrier Coating,” *Applied Thermal Engineering*, vol. 80, pp. 212-219, 2015. [CrossRef] [Google Scholar] [Publisher Link]

[13] A.K. Agarwal, J. Bijwe, and L.M. Das, “Effect of Biodiesel Utilization of Wear of Vital Parts in Compression Ignition Engine,” *Journal of Engineering for Gas Turbines and Power*, vol. 125, no. 2, pp. 604-611, 2003. [CrossRef] [Google Scholar] [Publisher Link]

[14] Sharad P. Jagtap, Anand N. Pawar, and Subhash Lahane, "Improving the Usability of Biodiesel Blend in Low Heat Rejection Diesel Engine through Combustion, Performance and Emission Analysis," *Renewable Energy*, vol. 155, pp. 628-644, 2020. [CrossRef] [Google Scholar] [Publisher Link]

[15] V. Karthickeyan et al., "Experimental Investigation of Pomegranate Oil Methyl Ester in Ceramic Coated Engine at Different Operating Condition in Direct Injection Diesel Engine with Energy and Exergy Analysis," *Energy Conversion and Management*, vol. 205, 2020. [CrossRef] [Google Scholar] [Publisher Link]

[16] Karthickeyan Viswanathan, B. Ashok, and Arivalagan Pugazhendhi, "Comprehensive Study of Engine Characteristics of Novel Biodiesel from Curry Leaf (Murraya Koenigii) Oil in Ceramic Layered Diesel Engine," *Fuel*, vol. 280, 2020. [CrossRef] [Google Scholar] [Publisher Link]

[17] V. Karthickeyan, "Effect of Cetane Enhancer on Moringa Oleifera Biodiesel in a Thermal Coated Direct Injection Diesel Engine," *Fuel*, vol. 235, pp. 538-550, 2019. [CrossRef] [Google Scholar] [Publisher Link]

[18] Uğur Öztürk, Hanbey Hazar, and Fikret Yılmaz, "Comparative Performance and Emission Characteristics of Peanut Seed Oil Methyl Ester (PSME) on a Thermal Isolated Diesel Engine," *Energy*, vol. 167, pp. 260-268, 2019. [CrossRef] [Google Scholar] [Publisher Link]

[19] S. Mohamed Abbas, and A. Elayaperumal, "Experimental Investigation on the Effect of Ceramic Coating on Engine Performance and Emission Characteristics for Cleaner Production," *Journal of Cleaner Production*, vol. 214, pp. 506-513, 2019. [CrossRef] [Google Scholar] [Publisher Link]

[20] I.T. Yilmaz, and M. Gumus, "Investigation of the Effect of Biogas on Combustion and Emissions of TBC Diesel Engine," *Fuel*, vol. 188, pp. 69-78, 2017. [CrossRef] [Google Scholar] [Publisher Link]

[21] Selman Aydın, and Cenk Sayın, "Impact of Thermal Barrier Coating Application on the Combustion, Performance and Emissions of a Diesel Engine Fueled with Waste Cooking Oil Biodiesel–Diesel Blends," *Fuel*, vol. 136, pp. 334-340, 2014. [CrossRef] [Google Scholar] [Publisher Link]

[22] Ekrem Buyukkaya, and Muhammet Cerit, "Experimental Study of NOx Emissions and Injection Timing of a Low Heat Rejection Diesel Engine," *International Journal of Thermal Sciences*, vol. 47, no. 8, pp. 1096-1106, 2008. [CrossRef] [Google Scholar] [Publisher Link]

[23] Adnan Parlak, "The Effect of Heat Transfer on Performance of the Diesel Cycle and Exergy of the Exhaust Gas Stream in a LHR Diesel Engine at the Optimum Injection Timing," *Energy Conversion Management*, vol. 46, no. 2, pp. 167-179, 2005. [CrossRef] [Google Scholar] [Publisher Link]

[24] Sukumar Puhan, "Mahua oil (Madhuca Indica Seed Oil) Methyl Ester as Biodiesel-Preparation and Emission Characterstics," *Biomass and Bioenergy*, vol. 28, no. 1, pp. 87-93, 2005. [CrossRef] [Google Scholar] [Publisher Link]

[25] N. Saravanan, G. Nagarajan, and Sukumar Puhan, "Experimental Investigation on a DI Diesel Engine Fuelled with Madhuca Indica Ester and Diesel Blend," *Biomass and Bioenergy*, vol. 34, no. 6, pp. 838-843, 2010. [CrossRef] [Google Scholar] [Publisher Link]

[26] H.R. Amriya Tasneem et al., "Ceramic Material for Thermal Barrier Coatings in Compression Ignition Engine for its Performance Evaluation with Biodiesel," *Materials Today: Proceedings*, vol. 46, no. 17, pp. 7745-7751, 2021. [CrossRef] [Google Scholar] [Publisher Link]

[27] P.K. Devan, and N.V. Mahalakshmi, "Performance, Emission and Combustion Characteristics of Poon Oil and its Diesel Blends in a DI Diesel Engine," *Fuel*, vol. 88, no. 5, pp. 861-867, 2009. [CrossRef] [Google Scholar] [Publisher Link]

[28] J. Narayana Reddy, and A. Ramesh, "Parametric Studies for Improving the Performance of a Jatropha Oil-Fuelled Compression Ignition Engine," *Renewable Energy*, vol. 31, no. 12, pp. 1994-2016, 2006. [CrossRef] [Google Scholar] [Publisher Link]

[29] S. Bari, C.W. Yu, and T.H. Lim, "Effect of Fuel Injection Timing with Waste Cooking Oil as a Fuel in a Direct Injection Diesel Engine," *Proceedings of the Institution of Mechanical Engineers, Part D. Journal of Automobile Engineering*, vol. 218, no. 1, pp. 93-104, 2004. [CrossRef] [Google Scholar] [Publisher Link]

[30] İsmet Çelikten, Atilla Koca, and Mehmet Ali Arslan, "Comparison of Performance and Emissions of Diesel Fuel, Rapeseed and Soybean Oil Methyl Esters Injected at Different Pressures," *Renewable Energy*, vol. 35, no. 4, pp. 814-820, 2010. [CrossRef] [Google Scholar] [Publisher Link]

[31] V. Arul Mozhi Selvan, R.B. Anand, and M. Udayakumar, "Combustion Characteristics of Diesohol Using Biodiesel as an Additive in a Direct Injection Compression Ignition Engine under Various Compression Ratios," *Energy & Fuels*, vol. 23, no. 11, pp. 5413-5422, 2009. [CrossRef] [Google Scholar] [Publisher Link]

[32] O.D. Hebbal, K. Vijayakumar Reddy, and K. Rajagopal, "Performance Characteristics of a Diesel Engine with Deccan Hemp Oil," *Fuel*, vol. 85, no. 14-15, pp. 2187-2194, 2006. [CrossRef] [Google Scholar] [Publisher Link]